

Table 2. The Values of Relaxation Spectra $H(\beta)$ Calculated from Stress Relaxation Curves for Nylon 6 in Air at 10°C, 20°C, 30°C and 40°C

ln β	β (sec)	$H(\beta) \times 10^{-5}$ (N/m ²)			
		10°C	20°C	30°C	40°C
-2	0.14	0.049	0.020	3.756	21.601
-1	0.37	0.132	0.055	9.663	41.231
0	1.00	0.359	0.150	22.971	62.492
1	2.72	0.973	0.407	46.772	77.536
2	7.39	2.631	1.105	76.241	85.220
3	20.09	7.048	2.980	99.923	88.476
4	54.59	18.435	7.925	113.113	89.743
5	148.41	45.482	20.259	118.957	90.218
6	403.43	99.144	48.217	121.275	90.359
7	1096.63	176.509	97.578	122.151	90.458
8	2980.96	249.591	157.864	122.469	90.472
9	8103.08	295.495	205.561	122.528	90.402
10	22026.47	316.217	231.016	122.117	89.833
11	59874.14	316.939	236.121	118.867	85.805
12	162754.79	269.696	201.141	98.893	63.782
13	442413.39	111.932	81.433	38.555	16.802
14	1202604.28	5.937	4.052	1.808	0.917

References

1. R. H. Blanc, *Rheol. Acta*, **27**, 482 (1988).

- J. D. Ferry, *Viscoelastic Properties of Polymers*, Wiley, New York (1980).
- B. H. Bersted, *J. Appl. Polym. Sci.*, **19**, 2167 (1975).
- M. Shida and R. N. Shroff, *Trans. Soc., Rheology*, **14**, 605 (1970).
- R. S. Lakes and S. Saha, *Science*, **104**, 501 (1979).
- R. S. Lakes and J. L. Katz, *J. Biomech.*, **104**, 501 (1979).
- N. W. Tschoegl, *Rheol. Acta*, **10**, 595 (1971).
- J. Stanislav and B. Hlavacek, *Trans. Soc. Rheol.*, **17**, 331 (1973).
- T. L. Smith, *J. Polym. Sci.*, **C35**, 39 (1971).
- T. Ree and H. Eyring, *J. Appl. Phys.*, **26**(7), 793 (1955).
- N. J. Kim, E. R. Kim, and S. J. Hahn, *Bull. Korean Chem. Soc.*, **12**, 468 (1991).
- T. Kunugi, I. Isobe, and K. Kimura, *J. Appl. Polym. Sci.*, **24**, 923 (1979).
- V. B. Gupta, C. Ramesh, and A. K. Gupta, *J. Appl. Sci.*, **29**, 4203 (1984).
- N. W. Tschoegl, *The Theory of linear Viscoelastic Behavior*, Academic Press, New York (1981).
- F. R. Schwarzl, *Pure Appl. Chem.*, **23**, 219 (1970).
- F. R. Schwarzl, *Rheol. Acta*, **9**, 382 (1970).
- T. Alfrey and P. Doty, *J. Appl. Phys.*, **16**, 700 (1945).
- J. D. Ferry and M. L. Williams, *J. Colloid Sci.*, **7**, 347 (1952).

Conducting Polypyrrole Doped with Hexacyanoferrate Anions: an Electrochemical and Spectroscopic Study

Junghee Han[†], Seungjun Lee[‡], and Woon-ki Paik^{*}

Department of Chemistry, Sogang University, Seoul 121-742. Received March 20, 1992

Conducting polypyrrole doped with iron (II, III) hexacyanate Fe(CN)₆^{z-} ions was studied for its physical and electrochemical properties. The polymer exhibited two pairs of waves in the cyclic voltammogram, one for the reversible oxidation/reduction of the incorporated iron hexacyanate ions and the other for the near-reversible oxidation/reduction of the polypyrrole moiety. The exchange of ions incorporated in the polymer and other ions present in solutions were examined by following the decrease of the reversible redox peaks of Fe(CN)₆^{z-}, and by EDX analysis. The spin density of this highly conducting polymer as probed by ESR spectroscopy was extremely low compared to polypyrrole doped with common anions.

Introduction

Conducting Polymers "doped" with various anions have attracted much interest in recent years. Although the main

characteristics of a conducting polymer is determined by the kinds of monomers and the linkage between the monomers in the polymer backbone, the doped anions sometimes impart significant influence on the physical and electrochemical properties of the conducting polymers.¹ While most of the anions are chemically inert charge compensators in the polymer structure with the polymer itself in the cationic form, anions with multiple oxidation states may actively participate in the oxidation/reduction reaction. Polymers with such anions,

[†] Present address: Central Research Laboratory, Korea Explosives Group, Taejon 302-345, Korea

[‡] Present address: R&D Department, Isu Chemical Company, Ltd., Onsan, Kyungnam 689-890, Korea

therefore, are expected to possess interesting properties. Iron (II, III) hexacyanate $\text{Fe}(\text{CN})_6^{z-}$ ions ($z=3, 4$) are such ions, which are also interesting because they are multiple-charged and thus may bestow unusual property to the polymer, and because these ions are fairly massive and therefore migration of these ions in the polymer matrix is expected to be unfavorable compared to small ions used as the dopant in conducting polymers. In this paper, synthesis of conducting polypyrrole (PPy) doped with $\text{Fe}(\text{CN})_6^{z-}$ ions by electropolymerization and the results of property examinations are reported.

Experimental

Chemicals and Solutions. Reagent grade chemicals were dissolved in purified water or acetonitrile (CH_3CN) to prepare the solutions. Acetonitrile (Fluka) was purified by distillation after refluxing with CaH_2 for two hours. Pyrrole (Aldrich) was also purified before use by distillation with CaH_2 to remove water and impurities. Water was purified by passing through columns of filters, adsorbent and ion exchange beds (Barnstead Nanopure II), which yielded water of the resistivity values higher than 10 Mohm-cm. The solutions used for the polymerization was mostly aqueous or acetonitrile solutions, 0.1 M in pyrrole and 0.1 M in $\text{K}_4\text{Fe}(\text{CN})_6$ as the electrolyte, except where specified otherwise. $\text{K}_4\text{Fe}(\text{CN})_6 \cdot (\text{H}_2\text{O})_3$ and other electrolytes were analytical reagent grade (from Aldrich and Fluka) and were used without purification. The solutions were deaerated by bubbling purified nitrogen before the synthesis and was shielded from oxygen contamination by passing nitrogen over the solution during the synthesis.

Cell and Equipment. A three-electrode glass cell was used for the electrochemical synthesis and voltammetric experiments. In the cell, the counter electrode compartment was separated from the working electrode compartment by a disk of fritted glass. The reference electrode, a saturated calomel (SCE) or a saturated sodium calomel electrode (SSCE), was placed in a tube with the Luggin capillary connected at the bottom. All the potentials reported in this paper are referred to SCE. A platinum plate of approximately 1 cm^2 surface area or platinum wire having approximately 0.3 cm^2 of surface area was used as the working electrode. A potentiostat and a potential programmer (EG & G) were used in the synthesis and the voltammetric experiments. Most of the experiments were conducted at room temperature. An ESR spectrometer (Bruker model ER200E) and a Hewlett-Packard frequency counter were used for the ESR study. Other equipment used include Elemental Analyzer (Perkin-Elmer 240C), Scanning Electron Microscope (JEOLJSM840A), EDX spectrometer (AN 1000), FT-IR (BrukerIFS-88), and a Thermal Analysis equipment system (Du Pont Data analysis System 9900, DSC 910).

Results and Discussion

Polymerization. From an aqueous solution containing the monomer and $\text{K}_4\text{Fe}(\text{CN})_6$, the cyclic voltammograms (CV) shown in Figure 1 were obtained. The curve from the first potential sweep is responsible for the potential scan on the bare Pt electrode in the presence of pyrrole, while the suc-

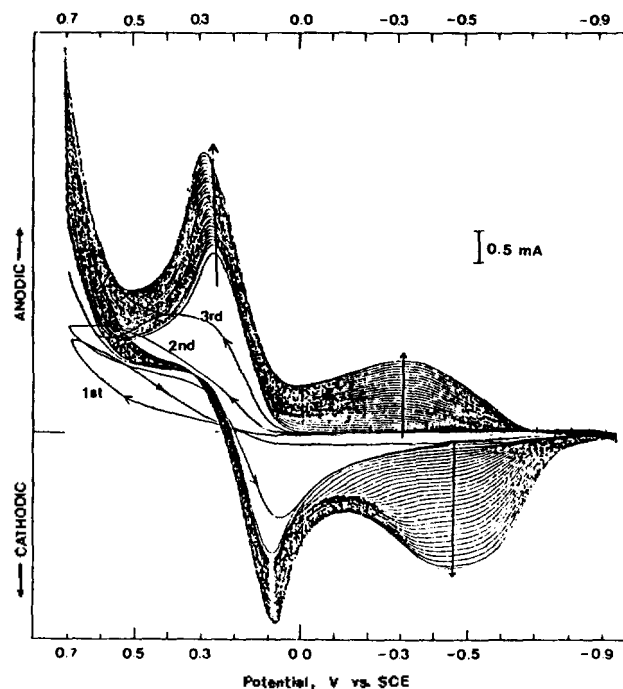


Figure 1. Cyclic voltammogram (CV) obtained during formation of polypyrrole in 0.1 M $\text{K}_4\text{Fe}(\text{CN})_6$ aqueous solution. Scan rate = 50 mV s^{-1} .

cessive curves are the CV's of the conducting polypyrrole film as they are formed on the Pt electrode and the thickness is increased with successive potential cycles. The voltammogram shows sharp oxidation-reduction peaks near 0.1-0.2 V vs SCE, corresponding to the reversible oxidation-reduction of ferrocyanide/ferricyanide couple in addition to the broad anodic and cathodic waves near -0.4 V responsible for the oxidation and reduction of polypyrrole. In the positive range of potential, polypyrrole is synthesized by electropolymerization doped with ferrocyanide [$\text{Fe}(\text{CN})_6^{3-}$] ions. On the negative potential sweep, the doped anion is reduced to ferrocyanide [$\text{Fe}(\text{CN})_6^{4-}$] ions, followed by reduction of the polymer itself at more negative potential. Hereafter, polypyrrole doped with $\text{Fe}(\text{CN})_6^{z-}$ ions will be denoted PPy- $\text{Fe}(\text{CN})_6$. The rate of polymerization, indicated by the growing wave heights, was much faster than with other anions such as Cl^- , ClO_4^- , or SO_4^{2-} . Synthesis of this same polymer by electropolymerization at the gas/solution interface (solution-surface polymerization method²) was also rapid and produced good film, as will be reported in a separate paper.

Polymer Properties. To obtain a polypyrrole film with a desired thickness, potentiostatic polymerization was mostly conducted with the potential fixed at 0.7 V. The polymer thus obtained was in the form of a black film which can be peeled off from the substrate electrode. The films were somewhat flexible and smooth to the bare eyes. Scanning electron microscopy (SEM) pictures revealed a highly porous structure in the film with globular appearance on the solution side. The cross-sectional SEM picture is shown in Figure 2. Differential scanning calorimetry (DSC) indicated that the glass transition temperature of PPy- $\text{Fe}(\text{CN})_6$ is 99°C whereas that of PPy- ClO_4 is 83°C. PPy- $\text{Fe}(\text{CN})_6$ was stable in wide range of temperature; no significant change was detected



(b) (a)

Figure 2. SEM photograph of cross section of PPy-Fe(CN)₆ film. (a) Side adjacent to electrode surface, (b) Side adjacent to solution.

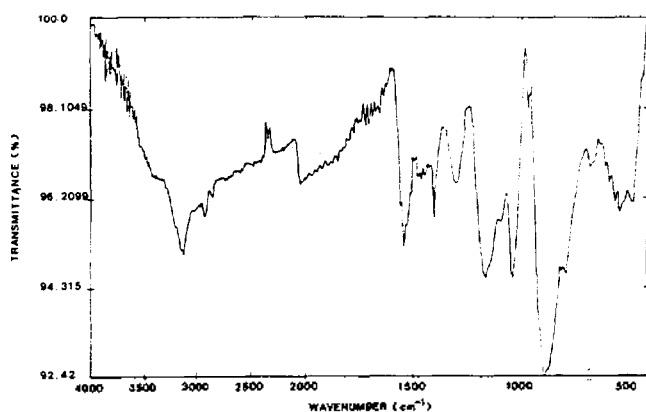


Figure 3. FT-IR spectrum of PPy-Fe(CN)₆.

in DSC up to 500°C. Weight decrease was indicated from 400°C by the thermogravimetric analysis (TGA). PPy-Fe(CN)₆ film was pulverized and pelleted with KBr for FT-IR spectroscopic measurement, the result of which is shown in Figure 4. The spectrum is close to those of other conducting polypyrroles except that absorption at 2050 cm⁻¹ appears which reveals the existence of CN groups.

Voltammetric Studies. If the monomer/electrolyte solution was replaced with a solution of electrolyte containing no Fe(CN)₆⁴⁻ and monomer after polymer film of ca. 100 μm was attained, the cyclic voltammogram of Figure 4(a) was obtained, which is to be compared with that of a polypyrrole doped with ClO₄⁻ ion, Figure 4(b). Here again, the CV of PPy doped with Fe(CN)₆⁴⁻ is characterized by the presence of the pair of reversible peaks in the positive potential range. Therefore, the pair of reversible peaks in the positive potential range is due to the oxidation/reduction of the Fe(CN)₆⁴⁻ ions doped in the polymer matrix, instead of Fe(CN)₆⁴⁻ ions present in the electrolyte solution.

The broad waves of PPy-Fe(CN)₆ film in the negative potential range responsible for the oxidation-reduction of the polypyrrole are somewhat less broad compared to the other polypyrrole conductors doped with simple anions, and are

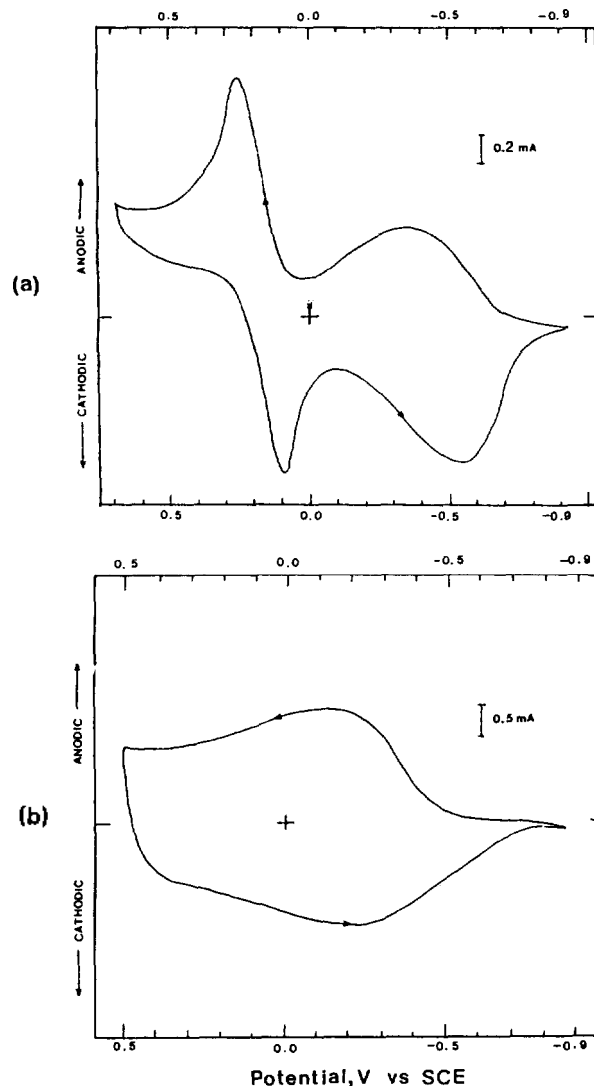


Figure 4. (a) CV of PPy-Fe(CN)₆; (b) CV of PPy-ClO₄. Solvent: water. Scan rate = 50 mV s⁻¹.

slightly shifted to the negative potential direction. This seems to indicate that in the polymer with Fe(CN)₆⁴⁻ ions, the redox behavior is less obscured by the capacitive charging waves that characterize the polymer doped with other ions. The shape of the CV of PPy-Fe(CN)₆ film was retained in solutions of electrolytes other than K₄Fe(CN)₆ for the initial few cycles. The shape changed gradually with repeated cycling of the potential depending on the kinds of electrolytes (see below).

Figure 5(a) is the CV obtained with the potential scan ranges limited within narrow ranges of the oxidation-reduction of the Fe(CN)₆⁴⁻ couple, and Figure 5(b) is the CV obtained within the potential range of oxidation-reduction of the polymer itself. The pair of peaks at the positive potential range (Figure 5(a)) is almost identical to that of the Fe(CN)₆⁴⁻ couple in the aqueous solution at a Pt electrode. The hexacyanoferrate ions are obviously trapped in the polymer matrix with the electrochemical properties unchanged. The CV's in Figure 5(b) at various scan rates show well-behaved, near-reversible redox property of the polypyrrole itself.

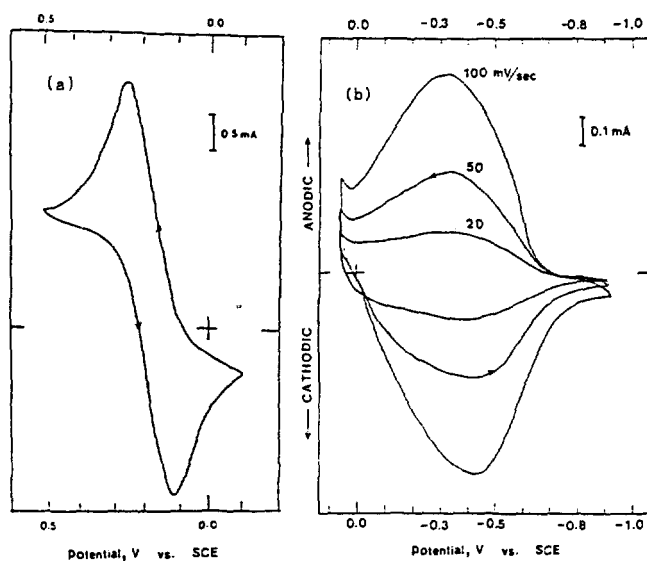


Figure 5. CV of PPy-Fe(CN)₆, (a) Potential scan range: -0.1-+0.5 V. Scan Rate=100 mV s⁻¹, (b) Scan range: -0.9+0.1 V.

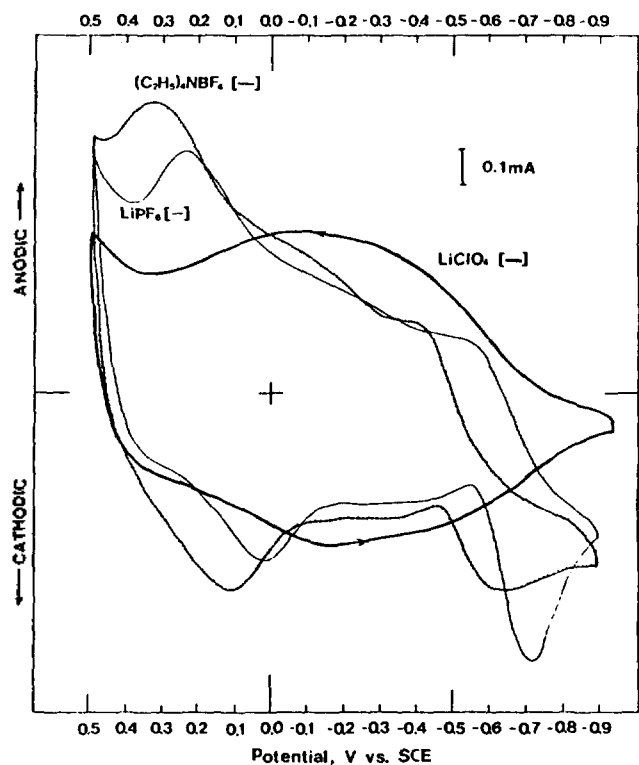


Figure 6. CV of PPy-Fe(CN)₆ in aqueous solutions containing various electrolytes. Scan rate=50 mV s⁻¹.

In order to examine the exchange of the doped ions and the consequent degradation of the reversible redox behavior of Fe(CN)₆²⁻, the electrode coated with PPy-Fe(CN)₆ film was placed in aqueous and acetonitrile solutions containing various electrolytes, and the cyclic potential scans were repeated for extended periods. The pair of Fe(CN)₆²⁻ peaks at the more positive potential of Figure 4(a) diminished gradually with repeated cycles to various extents depending on the electrolyte solutions. In Figure 6 are CV's obtained after

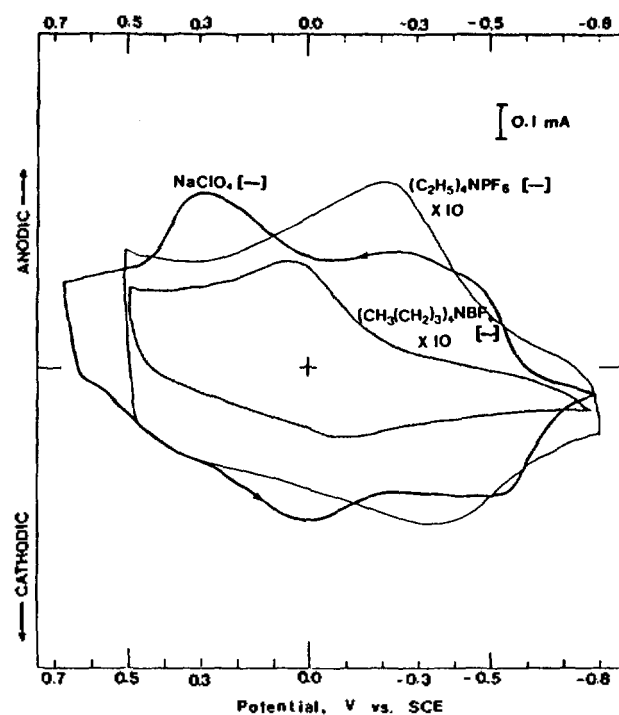


Figure 7. CV of PPy-Fe(CN)₆ in acetonitrile solutions containing various electrolytes. Scan rate=50 mV s⁻¹.

continuous cycling of the potential for 1 hour in aqueous solutions containing three different anions, ClO₄⁻, PF₆⁻, and BF₄⁻. The Fe(CN)₆²⁻ peaks diminished most markedly in LiClO₄ solution, while they remained in the other two electrolytes after more than 60 cycles of the potential scan during the 1 h period. The CV in the LiClO₄ solution resembles very much the CV of PPy-ClO₄ of Figure 4(b). Therefore, most of the Fe(CN)₆²⁻ ions originally associated with the cationic polymer were replaced with ClO₄⁻. Penetration of ClO₄⁻ ions into the polymer structure seems to be easy. On the other hand it can be seen that the other anions PF₆⁻ and BF₄⁻ in Figure 6 replaced only a fraction of Fe(CN)₆²⁻ ions in the polymer structure. The reduction waves appearing with PF₆⁻ and BF₄⁻ ions near the cathodic extremes are confirmed to be due to their reduction. We speculate that penetration of these two small ions into the polymer is energetically less favorable than ClO₄⁻ possibly due to their hydration in the aqueous phase.

In Figure 7 are shown the CV's obtained after 1 h of cycling in acetonitrile solutions of three different electrolytes. Contrary to the case of the aqueous solutions of Figure 6, the Fe(CN)₆²⁻ peaks are least diminished in NaClO₄ solution, while they completely disappeared in tetraalkylammonium salt solutions. Also, marked decrease in the oxidation-reduction currents occurred in these solutions. For the Fe(CN)₆²⁻ peaks to be preserved, the cations must migrate in and out of the polymer phase so that the charge neutrality is conserved without loss of Fe(CN)₆²⁻ from the polymer matrix during the oxidation and reduction. In the case when the solvent is acetonitrile, the organic cations seem to be unlikely to leave the organic solvent to go into the polymer phase, and thus Fe(CN)₆²⁻ ions are expelled. Comparison of the effect of different cations is made also in Figure 8 where CV's

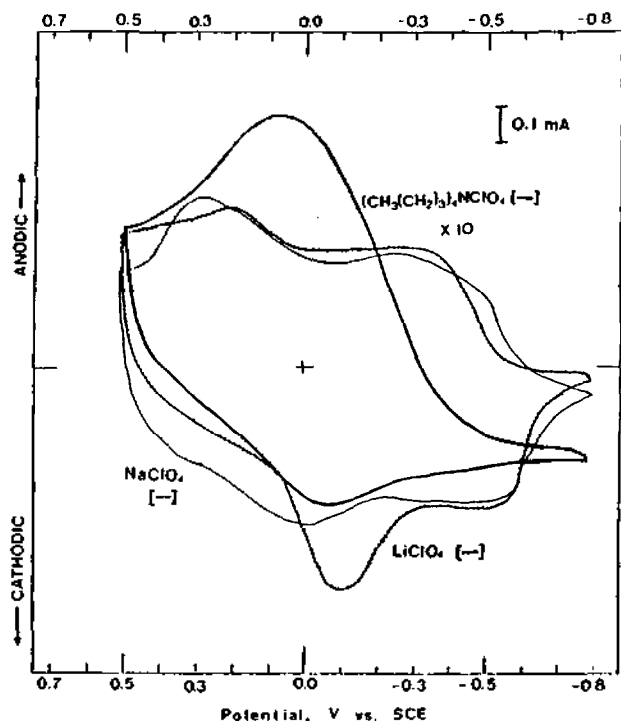


Figure 8. CV of PPy-Fe(CN)₆ in acetonitrile solutions containing various cations. Scan rate = 50 mV s⁻¹.

in three different electrolytes with common ClO₄⁻ ion are shown. Here also the removal of Fe(CN)₆⁴⁻ seems to be more complete in solutions of the organic cation salts. CV with LiBF₄ (not shown in the figures for clarity) indicated that the removal of Fe(CN)₆⁴⁻ was less complete than in [CH₃(CH₂)₃]₄NBF₄ solution. From all of the above evidences it can be concluded that the replacement of Fe(CN)₆⁴⁻ ions in PPy-Fe(CN)₆ is strongly influenced by the mobility of cations and anions in the polymer structure and through the solution/polymer interface. The interdependence of the relative ease of ion movements in PPy was studied by Naoi *et al.*³ by the quartz crystal microbalance method. They observed that only anions move in the polymer on oxidation and reduction of PPy doped with small anions, cations only move in PPy with polymer anions, and both anion and cation movements are possible in PPy with medium-sized anions. For possible applications of PPy-Fe(CN)₆, perhaps in battery electrode or in other charge storage devices, preservation of Fe(CN)₆⁴⁻ ions in the polymer phase will be beneficial. It will be advantageous for such applications to have anions in the environment that are not easily removed from the solution and have small mobilities in the polymer. Also advantageous will be to have cations that can readily leave the solvent to go into the polymer and migrate easily in the polymer.

Conductivity. To measure the conductivity of the polymer as a function of the potential at which it was equilibrated, the samples of PPy-Fe(CN)₆ film to be measured for its conductivity was taken out of the solution in which it had been potentiostated at various potentials after stopping the potential scan while it was in the negative-going scan phase. The potentiostat was switched off immediately before the film was taken out of the solution. The film was then peeled off from the electrode, rinsed with deionized water,

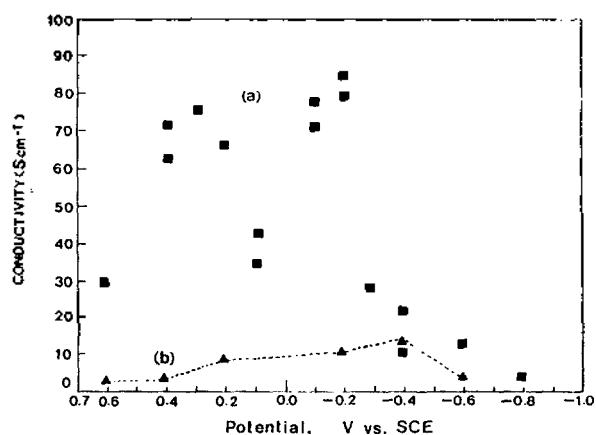


Figure 9. Conductivity of PPy-Fe(CN)₆ film specimen equilibrated at various potentials before taking out of the solution. (a) Fresh specimen, measured within an hour after preparation, (b) Specimen aged for 1 month.

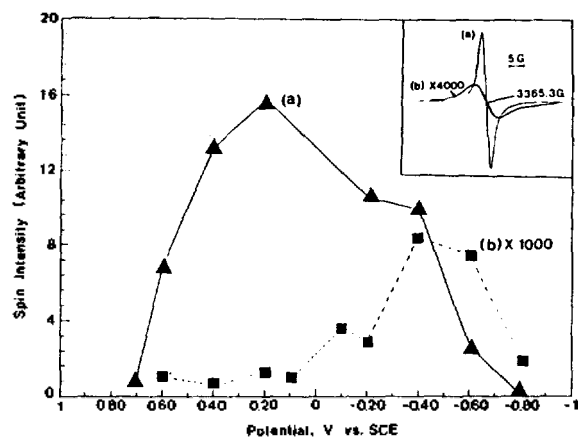


Figure 10. ESR signal intensity of (a) PPy-ClO₄ and (b) PPy-Fe(CN)₆ film specimen equilibrated at various potentials before taking out of the solution. Inset: esr spectrum of PPy-Fe(CN)₆ (b), compared with that of PPy-ClO₄ (a).

and was dried in a vacuum-oven for about a day before the conductivity was measured by the four-probe method. As shown in Figure 9, the conductivity-potential curve had double humps, with high conductivities near 0.4 V and -0.2 V. Thus it appears that the conductivity is high when both PPy and Fe(CN)₆⁴⁻ are in the fully oxidized form or when the ions are reduced to Fe(CN)₆⁴⁻. The conductivity is somewhat smaller between 0.1-0.2 V, where the anions are partly in Fe(CN)₆³⁻ form and partly in Fe(CN)₆⁴⁻ form according to the CV in Figure 4(a). The reason for this dip in the conductivity with the mixed valency of the anion is not understood at the present.

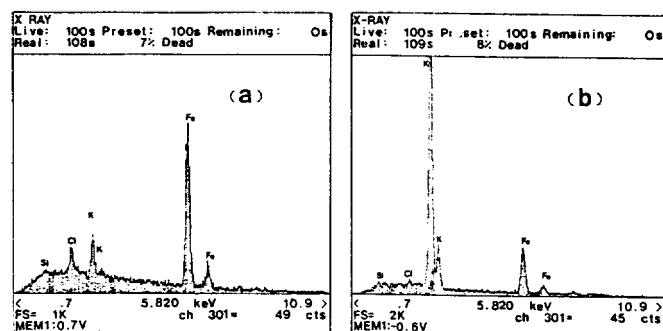
ESR and Spin Density. Figure 10 shows ESR signal intensities of PPy-Fe(CN)₆ and PPy-ClO₄ polymers as functions of the electrode potential. The specimen used in this experiment was also prepared in the same manner as for the conductivity measurement. The ESR intensity-potential relation for PPy-ClO₄ polymer is in agreement with that obtained by Nechtschein *et al.*⁴ from an *in situ* experiment in acetonitrile solution. A typical ESR spectrum of PPy-Fe(CN)₆ is compared with that of PPy-ClO₄ in the inset of Figure

Table 1. Relative Mole Abundance Ratio of C H N Elements and the Composition of PPy-Fe(CN)₆ Polymer at Different Potentials

Element Potential	(C ₄ H ₃ N) _x Fe(CN) ₆ ·yH ₂ O				
	C	H	N	x	y
+0.70 V	1.00	0.881	0.366	8.2	4.79
-0.60 V	1.00	0.813	0.329	12.7	4.04

10. The ESR signal intensity of PPy-Fe(CN)₆ is extremely small throughout the whole potential compared to that of PPy-ClO₄ (Note that the spin density scale for PPy-Fe(CN)₆ in Figure 10 is multiplied by a factor of 1000). Contrary to the behavior of PPy-ClO₄, and polypyrrole samples doped with other anions^{5,6} the ESR signal of PPy-Fe(CN)₆ is even smaller at more anodic potentials where greater conductivity is observed. It is generally accepted that when PPy doped with common anions is moderately oxidized and conducting, it has larger spin density and hence exhibit larger ESR intensity, and when it is over-oxidized the intensity decreases due to formation of bipolarons^{4,7,8} because a bipolaron does not have spin. Therefore, the behavior of PPy-Fe(CN)₆ appears peculiar. It can be reasoned that the presence of Fe(CN)₆⁴⁻ ions in the polymer is very effective in inducing formation of bipolarons. The merging of two polarons to form a bipolaron is believed to be somewhat hindered in many conducting polymers by the coulombic repulsion between the positive charges of the polarons. However, when the polymer is associated with Fe(CN)₆⁴⁻ ions each of which has triple or quadruple negative charge, formation of bipolarons can be favorable electrostatically. In a "twisted" or "spiraled" structure of PPy backbone as proposed by Vork and Janssen⁹, the multi-charged spherically symmetric complex anions will be surrounded by the polymer chain in such a way that can diminish repulsion between positive charges of two polarons, pull them together and thus facilitate formation of bipolarons. We also observed, in a separate experiment in which polypyrrole was doped with CoCl₄²⁻ ions from acetonitrile solution, that the ESR signal intensity diminished drastically when the concentration of CoCl₄²⁻ ions in the solution increased. The ESR signal intensity slightly increased with aging of the PPy-Fe(CN)₆ specimen in the air, which is also contrary to the trends of other conducting polymers. Street *et al.*^{10,11} also reported that electrochemically cycled PPy did not show ESR spectrum, and suggested formation of spinless bipolarons.

Elemental Ratio. Sample PPy-Fe(CN)₆ polymer synthesized from aqueous K₄Fe(CN)₆ solution were equilibrated in the solution by fixing the electrode potential at +0.7 V or -0.7 V and then was analyzed for the contents of carbon, hydrogen and nitrogen. Results of the CHN analysis are summarized in Table 1 as the relative molar abundance ratio of the three elements at each potential. From the ratio of nitrogen to carbon, number of pyrrole monomer units for each Fe(CN)₆⁴⁻ ion, *x*, is calculated. An abundance value of hydrogen over that expected for (C₄H₃N)_xFe(CN)₆ formula is considered to be from water remaining in the sample. The samples were dried in a vacuum oven before the elemental analysis. However, it was reported that polypyrrole sam-

**Figure 11.** EDX spectra of PPy-Fe(CN)₆ film specimen equilibrated at (a) +0.7 V and (b) -0.6 V.

ples are difficult to dehydrate completely even with drying in vacuum or with heating at reduced pressure.^{9,12} With formula (C₄H₃N)_xFe(CN)₆·yH₂O, the number of pyrrole units to one Fe(CN)₆⁴⁻ ion is represented by *x* and the number of water molecule is represented by *y*, and these numbers are tabulated in the table.

The *x* value 8.2 obtained at +0.70 V, where the polymer is fully doped, corresponds at 8.2/3 ≅ 2.7 monomer units to a single negative charge because at this potential the cyanoferrate ion has triple negative charges. The number of monomer units to a singly charged anion in the fully doped state is known to be about 3-4 for small anions^{1,13,14} and slightly above 2 for large *p*-toluenesulfonate ion.⁹ The above number 2.7 is smaller than the typical figures. The multiple charges on the anion seem to make the average distance between the positive charge in the polymer backbone shorter, thus facilitating formation of bipolarons as discussed above in connection with the observed low spin density. The moderate increase in *x* value to 12.7 at -0.60 V reflects the fact that the anions are only partially released from the polymer matrix on reduction.

Unlike in conducting polymers with small anions in which the anions migrate out of the polymer on reduction, in PPy-Fe(CN)₆ the anions are not released easily from the polymer matrix into the solution as discussed above. Therefore, the cations must migrate in and out of the polymer to maintain the charge neutrality. This is confirmed by the results of Energy Dispersive X-ray (EDX) analysis of the PPy-Fe(CN)₆ film presented in Figure 11. The two EDX charts were obtained from samples equilibrated with K₄Fe(CN)₆ solutions at the electrode potentials of +0.70 V and -0.60 V. The relative abundance of K is very small at the anodic potential indicating that a small amount of K⁺ is present in the doped polymer, whereas at the cathodic potential K content is markedly increased because large amount of K⁺ is now transported into the polymer. Fe content is slightly decreased at the cathodic potential (Note that the scale in Figure 11(b) is twice that of Figure 11(a)). The small peaks of Cl and Si are considered to be from impurity. The ease of K⁺ ion migration (and possibly of other cations) and the difficulty of Fe(CN)₆⁴⁻ ion migration is responsible for retaining of Fe(CN)₆⁴⁻ ions in the polymer after repeated potential cycles in some of the cases examined above.

Acknowledgement. The SEM and EDX analyses were carried out with the help of Y. Kang and Y. Koh. FT-IR,

thermal analysis, and ESR measurements were helped by W. Yon, Y. Kim, and H. Kim, respectively. We acknowledge financial supports from the Ministry of Education and Korea Science and Engineering Foundation.

References

1. M. Salmon, A. F. Diaz, A. J. Logan, M. Krounbi, and J. Bargon, *Mol. Cryst. Liq. Cryst.*, **83**, 1297 (1983).
2. (a) E. H. Song, J. K. Chon, and W. Paik, *Bull. Korean Chem. Soc.*, **9**, 43 (1988); (b) E. H. Song, J. K. Chon, and W. Paik, *ibid.*, **11**, 41 (1990).
3. K. Naoi, M. Lien, and H. Smyrl, *J. Electrochem. Soc.*, **138**, 440 (1991).
4. M. Nechtschein, F. Devreux, F. Genoud, E. Vieil, J. M. Pernaut, and E. Genies, *Synthetic Metals*, **15**, 59 (1986).
5. S. Dong, J. Dings, and R. Zhan, *J. Chem. Soc., Faraday Trans. I*, **85**, 1599 (1989).
6. W. J. Albery and C. C. Jones, *Faraday Discuss. Chem. Soc.*, **78**, 193 (1984).
7. E. M. Genies and J. M. Pernaut, *J. Electroanal. Chem.*, **191**, 111 (1985).
8. F. Devreux, F. Genoud, M. Nechtschein, and B. Villeret, *Synth. Met.*, **18**, 89 (1987).
9. F. T. A. Vork and L. J. J. Janssen, *Electrochim. Acta*, **33**, 1513 (1988).
10. J. C. Scott, P. Pfluger, M. T. Krounbi, and G. B. Street, *Phys. Rev. B*, **28**, 2140 (1983).
11. J. L. Bredas, J. C. Scott, K. Yakushi, and G. B. Street, *ibid. B*, **30**, 1023 (1984).
12. K. J. Wynne and G. B. Street, *Macromolecules*, **18**, 2361 (1985).
13. E. M. Genies, G. Bideu, and A. Diaz, *J. Electrochem. Soc.*, **149**, 101 (1983).
14. S. Asavapiriyant, G. K. Chandler, G. A. Chandler, G. A. Gunawardena, and D. Pletcher, *J. Electroanal. Chem.*, **177**, 229 (1984).

Substitutional Effects of Na in the $\text{YBa}_2\text{Cu}_3\text{O}_{7-y}$ Oxide Superconductors

Nam Hwi Hur*, Dong Han Ha, Yong Ki Park, and Jong Chul Park

Korea Research Institute of Standards and Science, P.O.Box 3, Daedeog-Danji, Taejeon 305-606

Received March 20, 1992

Sodium substituted samples of $\text{Y}_{1-x}\text{Na}_x\text{Ba}_2\text{Cu}_3\text{O}_{7-y}$ for $0.00 \leq x \leq 0.16$ were prepared and characterized by X-ray powder pattern, electrical resistivity and magnetic susceptibility measurements, Raman spectroscopy, and idometric titration. The Na substituted compounds have narrow solid solution limits where $0.00 \leq x \leq 0.16$. As the Na concentration increases, the parent orthorhombic structure tends to gradually change to tetragonal. Small changes in the superconducting transition temperature, T_c , are observed in this solid solution region. Raman spectra for the Na phases are virtually identical with that of $\text{YBa}_2\text{Cu}_3\text{O}_7$ except that the Cu(1)-O(4) stretching mode at 504 cm^{-1} and the Cu(2)-O(2,3) bending mode at 340 cm^{-1} for $x=0.16$ are slightly shifted. The hole concentrations of the sodium substituted compounds ranged from 0.31 to 0.33 per Cu site are increased with Na content. The substitution of Na^+ for Y^{3+} site appears to create oxygen vacancies in the Cu-O chains, causes structural change from orthorhombic to tetragonal, and increases hole concentration in the substituted system.

Introduction

Following the discovery of superconductivity in $\text{YBa}_2\text{Cu}_3\text{O}_7$ (hereafter YBCO) by Wu *et al.*¹, there have been a lot of research on the substitutional effects on almost all sites in the compound². These are mainly concerned with possible isolation of new high T_c superconducting phases as well as investigation of the physical properties caused by the substitutions. It has been known that substitution of Y^{3+} in YBCO by most trivalent rare earth elements has little effect on the superconducting properties³. This suggests that interactions between superconducting electrons and magnetic moments of the rare earth ions are relatively negligible even if the effective magnetic moments are changed by employing various isovalent cations⁴. In the case of the $\text{Y}_{1-x}\text{Pr}_x\text{Ba}_2\text{Cu}_3\text{O}_{7-y}$ compound, however, the superconductivity is severely suppressed as Pr concentration increases⁵. This anomalous

behavior in the Pr substituted YBCO is believed to be related to the mixed valent state of Pr ions (Pr^{3+} and Pr^{4+}), in which f electrons contributed by the Pr ion cause superconducting pair breaking in the Pr substituted compounds. These results prompt us to investigate the substituted YBCO system where the interlayer cation site (Y^{3+}) is replaced with other nonisovalent cations.

Sodium substituted compounds of the type $\text{Y}_{1-x}\text{Na}_x\text{Ba}_2\text{Cu}_3\text{O}_{7-y}$ have been prepared by solid state reaction. Since the ionic size of monovalent Na^+ is almost identical with that of trivalent Y^{3+} , the Na^+ ion is expected to be substituted into Y^{3+} site without much effect on the structural integrity in the parent orthorhombic YBCO structure. From the structural standpoint, distortions in the sodium substituted phases might be expected to be negligible due to the small change in ionic radii. Structural distortions in the ABO_3 type perovskite structures are normally estimated by the value of toler-